AMERICAN SOCIETY FOR MICROBIOLOGY | Infection and Immunity®

BACTERIAL INFECTIONS

# *Scnn1b*-Transgenic BALB/c Mice as a Model of *Pseudomonas aeruginosa* Infections of the Cystic Fibrosis Lung

**Kristen J. Brao,[a,b] Brendan P. Wille,[a] Joshua Lieberman,[c] Robert K. Ernst,[a,b] Mark E. Shirtliff,[a,b†] Janette M. Harro[a]**

[a]Department of Microbial Pathogenesis, University of Maryland School of Dentistry, Baltimore, Maryland, USA
[b]Department of Molecular Microbiology and Immunology, University of Maryland School of Medicine, Baltimore, Maryland, USA
[c]Division of Microbiology, Department of Laboratory Medicine, University of Washington, Seattle, Washington, USA

**ABSTRACT** The opportunistic pathogen *Pseudomonas aeruginosa* is responsible for much of the morbidity and mortality associated with cystic fibrosis (CF), a condition that predisposes patients to chronic lung infections. *P. aeruginosa* lung infections are difficult to treat because *P. aeruginosa* adapts to the CF lung, can develop multidrug resistance, and can form biofilms. Despite the clinical significance of *P. aeruginosa*, modeling *P. aeruginosa* infections in CF has been challenging. Here, we characterize *Scnn1b*-transgenic (Tg) BALB/c mice as *P. aeruginosa* lung infection models. *Scnn1b*-Tg mice overexpress the epithelial $Na^+$ channel (ENaC) in their lungs, driving increased sodium absorption that causes lung pathology similar to CF. We intranasally infected *Scnn1b*-Tg mice and wild-type littermates with the laboratory *P. aeruginosa* strain PAO1 and CF clinical isolates and then assessed differences in bacterial clearance, cytokine responses, and histological features up to 12 days postinfection. *Scnn1b*-Tg mice carried higher bacterial burdens when infected with biofilm-grown rather than planktonic PAO1; *Scnn1b*-Tg mice also cleared infections more slowly than their wild-type littermates. Infection with PAO1 elicited significant increases in proinflammatory and Th17-linked cytokines on day 3. *Scnn1b*-Tg mice infected with nonmucoid early CF isolates maintained bacterial burdens and mounted immune responses similar to those of PAO1-infected *Scnn1b*-Tg mice. In contrast, *Scnn1b*-Tg mice infected with a mucoid CF isolate carried high bacterial burdens, produced significantly more interleukin 1$\beta$ (IL-1$\beta$), IL-13, IL-17, IL-22, and KC, and showed severe immune cell infiltration into the bronchioles. Taken together, these results show the promise of *Scnn1b*-Tg mice as models of early *P. aeruginosa* colonization in the CF lung.

**KEYWORDS** *Pseudomonas aeruginosa*, cystic fibrosis, mouse model

*Pseudomonas aeruginosa* is an opportunistic pathogen and important causative agent of serious lung infections in hospitalized and immunocompromised patients. These infections are difficult to treat, because *P. aeruginosa* can develop multidrug resistance and is capable of forming biofilms. Biofilms are microbial communities encased in a matrix of extracellular proteins, nucleic acids, and polysaccharides (1). Bacteria growing as a biofilm can tolerate antibiotic exposure and resist clearance by the host immune system (2), resulting in the establishment of chronic infections. *P. aeruginosa* is also metabolically adaptable and capable of producing a variety of virulence factors, enabling it to survive in the environment as well as human hosts.

Mice infected with planktonic *P. aeruginosa* develop acute pneumonia, resulting in sepsis or rapid clearance of the bacteria (3, 4). Acute pneumonia models have been valuable for the identification of *P. aeruginosa* virulence factors, including flagella (5) and pili (6), a type III secretion system, and secreted exotoxins (7), proteases (8), and phenazines (9, 10). To mimic a chronic lung infection, *P. aeruginosa* has been embed-

**Citation** Brao KJ, Wille BP, Lieberman J, Ernst RK, Shirtliff ME, Harro JM. 2020. *Scnn1b*-transgenic BALB/c mice as a model of *Pseudomonas aeruginosa* infections of the cystic fibrosis lung. Infect Immun 88:e00237-20. https://doi.org/10.1128/IAI.00237-20.

**Editor** Manuela Raffatellu, University of California San Diego School of Medicine



Address correspondence to Robert K. Ernst, rkernst@umaryland.edu, or Janette M. Harro, jharro@umaryland.edu.

† Deceased.

**Received** 23 April 2020
**Returned for modification** 17 June 2020
**Accepted** 30 June 2020

**Accepted manuscript posted online** 6 July 2020
**Published** 19 August 2020

ded in an alginate/agarose bead (11, 12) or a fibrin plug (13, 14) that serves as an artificial biofilm and a long-term nidus of infection. Chronic *P. aeruginosa* lung infection models, which can prolong infection for up to 3 months (15), have been useful for testing anti-*P. aeruginosa* therapeutics (16, 17) and contributed to the understanding of the immune responses to chronic infection. For example, agar bead models have suggested that Th2-skewed immune responses increase susceptibility to infection (18), raising the possibility that immunomodulatory therapy could be beneficial.

*P. aeruginosa* is responsible for much of the lung function deterioration associated with cystic fibrosis (CF) (19), and by age 20, 60 to 70% of CF patients are intermittently colonized by *P. aeruginosa* (20). CF is an autosomal recessive genetic disease caused by defects in the production and function of the cyclic AMP-regulated cystic fibrosis transmembrane conductance regulator (CFTR) channel, resulting in disruption of chloride and bicarbonate transport across epithelial cells. Without proper ion transport, CF patients develop thick, dehydrated mucus and impaired mucociliary clearance in their airways, predisposing patients to recurrent and chronic lung infections. Early in CF patients' lives, *P. aeruginosa* infections are treatable with aggressive antibiotic regimens (21), but over time, *P. aeruginosa* adapts to the CF lung environment, typically through losing specific virulence factors while becoming increasingly antibiotic resistant (22, 23). Once a chronic infection is established, it is nearly impossible to eliminate.

Mucoid strains of *P. aeruginosa* hyperproduce the polysaccharide alginate and form thick biofilms. Mucoid *P. aeruginosa* is rarely observed in nature (24) but is selected through environmental adaptation within the CF lung (25, 26). The emergence of mucoid *P. aeruginosa* is linked to pulmonary exacerbations (27), coinfection with *Staphylococcus aureus* (28), increased antibiotic tolerance (29), resistance to opsonization and phagocytosis (30, 31), and worsened lung function deterioration (32). Although much progress has been made in treating the multisystem complications of CF, preventing and treating lung colonization with *P. aeruginosa* remains a major challenge.

A significant impediment to the study of CF lung infections is the lack of a CFTR mutant mouse that reliably develops the mucus plugging, neutrophil recruitment, and bronchiectasis observed in CF patients (33, 34). CFTR regulates the function of the epithelial $Na^+$ channel (ENaC), and these channels together largely control the flux of sodium and chloride across epithelium (35). When CFTR is defective in CF airways, ENaC is overactive, resulting in increased sodium absorption (36). To attempt to mimic airway mucus obstruction and test the hypothesis that increased sodium absorption would produce CF-like lung pathology in mice, Mall et al. (37) developed transgenic mice that overexpress the beta subunit of ENaC (gene *Scnn1b*) under the control of the club cell secretory protein promoter. These *Scnn1b*-transgenic (Tg) C57BL/6 and BALB/c mice show increased sodium absorption in the airways, which drives airway surface liquid dehydration, mucus obstruction, and neutrophilic inflammation, much like pathological observations in CF patients (37, 38). To date, *Scnn1b*-Tg mice have primarily been used to study the pathophysiology and treatment of CF-like muco-obstructive lung disease (39–42), but they have also shown promise as models for acute infections in CF-like lungs. Neonatal *Scnn1b*-Tg C3H $\times$ C57BL/6 mice have been shown to clear intratracheal infections with *Haemophilus influenzae* or *P. aeruginosa* more slowly than wild-type mice, but the infections have not been studied for longer than 3 days (37). *Scnn1b*-Tg C57BL/6 mice have also been infected with *P. aeruginosa* using a fibrin plug model to study mechanisms by which treatment with nebulized alpha-1 antitrypsin improves lung function and decreases *P. aeruginosa* burden in CF patients (14). That study was limited to the first 3 days of infection, so it did not address the chronic nature of CF lung infections, but it demonstrated the potential utility of *Scnn1b*-Tg mice for testing therapeutics against infections in a CF-like lung.

Here, we developed a model of CF lung infection with *P. aeruginosa* using *Scnn1b*-Tg BALB/c mice. This model uses an intranasal route of infection and does not embed bacteria in foreign substances to prevent clearance, similar to natural infections. An advantage of this model is its ease of use, permitting the study of *P. aeruginosa* in a

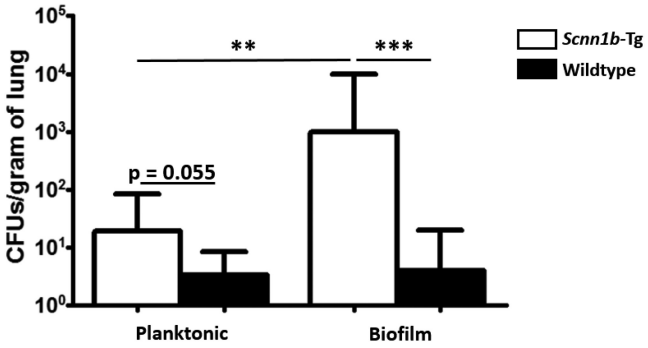


**FIG 1** Planktonic PAO1 is less infectious than PAO1 grown as a biofilm. PAO1 consistently colonizes the *Scnn1b*-Tg mouse lung when it is grown as a biofilm prior to infection rather than grown planktonically. *Scnn1b*-Tg mice and wild-type littermates were intranasally infected with $2 \times 10^6$ to $4 \times 10^6$ CFU planktonic PAO1 or $3 \times 10^6$ to $5 \times 10^6$ CFU biofilm-grown PAO1. Bars show geometric means with 95% confidence intervals. CFU data were log transformed and then analyzed using 2-tailed *t* tests. The limit of detection is 100 CFU/g of lung. Results are from independent planktonic infections (data from 4 infections; total of 24 wild-type and 27 *Scnn1b*-Tg mice) and biofilm infections (data from 3 infections; total of 11 wild-type and 10 *Scnn1b*-Tg mice). **, $P < 0.01$; ***, $P < 0.001$.

mouse with CF-like lung disease for up to 12 days postinfection. The utility of this model was confirmed by infecting mice with *P. aeruginosa* PAO1 as well as clinical isolates from young children with CF and evaluating clearance rates, bacterial burdens, and the immune response.

## RESULTS

**PAO1 consistently colonizes *Scnn1b*-Tg mouse lungs when it is grown as a biofilm.** To determine whether planktonic or biofilm-grown PAO1 was important in the colonization of the lung, *Scnn1b*-Tg mice and their wild-type littermates were intranasally infected with $2 \times 10^6$ to $4 \times 10^6$ CFU of planktonic or $3 \times 10^6$ to $5 \times 10^6$ CFU of biofilm-grown PAO1 on day 0. The biofilm inoculum was homogenized prior to plating, which was confirmed to break up bacterial aggregates using microscopy (see Fig. S1B in the supplemental material). On day 7 postinfection, more planktonically grown bacteria were recovered from *Scnn1b*-Tg mice than from wild-type mice ($P = 0.055$) (Fig. 1); however, only 41% (11/27) of surviving *Scnn1b*-Tg mice maintained the infection (geometric mean bacterial burden was below the limit of detection). In contrast, when PAO1 was grown as a biofilm, 90% (9/10 mice) of surviving *Scnn1b*-Tg mice remained infected on day 7, and they carried significantly more bacteria (geometric mean of 1,008 CFU/g of lung; $P = 0.006$). Among wild-type mice, only 25% (6/24 mice) and 27% (3/11 mice) remained infected on day 7 when infected with planktonic or biofilm-grown PAO1, respectively, demonstrating that the mucus-obstructed *Scnn1b*-Tg mice are more susceptible to infection with PAO1.

***Scnn1b*-Tg mice clear PAO1 infections more slowly than wild-type littermates.** To assess clearance rates of biofilm-grown PAO1, *Scnn1b*-Tg mice and their wild-type littermates were intranasally infected with $3 \times 10^6$ to $5 \times 10^6$ CFU. Mice were sacrificed on days 3, 7, and 12 postinfection. The bacterial load in the lungs declined over time for both wild-type and *Scnn1b*-Tg mice; however, *Scnn1b*-Tg mice cleared the infections more slowly than wild-type littermates (Fig. 2). On day 3, 100% of surviving *Scnn1b*-Tg and wild-type mice were infected: *Scnn1b*-Tg mice carried a geometric mean of 4,235 CFU/g of lung, whereas wild-type mice carried only 705 CFU ($P = 0.034$). Between days 3 and 7, wild-type mice cleared 99.5% of the bacteria in their lungs, compared to 76% in *Scnn1b*-Tg mice. By day 12, only 18% (2/11) of wild-type mice remained infected, compared to 50% (5/10) of *Scnn1b*-Tg mice. The mortality rates for the *Scnn1b*-Tg and wild-type mice were 21% and 3%, respectively ($P = 0.020$) (Fig. S2A). Mortality was limited to the first 3 days postinfection, and preliminary experiments suggested that mortality was a result of sepsis (determined by dissemination to the kidneys; data not shown). Both *Scnn1b*-Tg and wild-type mice lost weight following infection and then

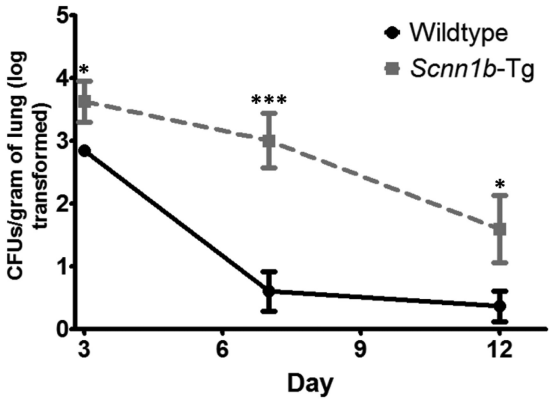


**FIG 2** *Scnn1b*-Tg mice clear PAO1 more slowly than wild-type littermates. Biofilm-grown PAO1 is cleared from *Scnn1b*-Tg lungs over 12 days of infection. *Scnn1b*-Tg and wild-type BALB/c mice were infected with $3 \times 10^6$ to $5 \times 10^6$ CFU PAO1 and sacrificed on days 3, 7, and 12 postinfection. Values are log-transformed numbers of CFU with standard errors of the means. CFU data were log transformed and compared using unpaired, two-tailed *t* tests. The limit of detection is 100 CFU/g of lung. Results are from independent infections (data from 3 infections; total of 34 wild-type mice and 38 *Scnn1b*-Tg mice). *, $P < 0.05$; ***, $P < 0.001$.

rebounded (Fig. S2B). No significant differences were found between male and female mice.

**Cytokine analysis.** Sputum samples from CF patients have been reported to contain large amounts of interleukin 17 (IL-17) during pulmonary exacerbations (43). To determine if *Scnn1b*-Tg BALB/c mice generate Th1-, Th2-, or Th17-skewed responses to *P. aeruginosa* infection and compare the response to that observed in CF patients, cytokine production in the lungs of *Scnn1b*-Tg and wild-type mice was compared on days 3 and 7 postinfection. Compared to wild-type mice, *Scnn1b*-Tg BALB/c mice produced increased levels of the Th1 cytokine gamma interferon (IFN-$\gamma$) and the neutrophil chemoattractant KC at baseline ($P = 0.037$ and 0.040), as well as on day 3 (postinfection ($P = 0.013$ and 0.049) (Fig. 3; Table S1). On day 3 postinfection, both *Scnn1b*-Tg and wild-type mice showed significantly increased production of IFN-$\gamma$ over mock-infected controls ($P = 0.003$ and 0.005); however, production of IL-12 p70, another Th1-associated cytokine, was unaffected. The Th2-associated cytokines IL-4 and IL-13 were not significantly increased by *P. aeruginosa* infection. In contrast, the proinflammatory cytokines IL-1$\beta$ and IL-6, as well as the Th17-associated cytokine IL-22, were significantly induced by *P. aeruginosa* infection on day 3 in both *Scnn1b*-Tg and wild-type mice (IL-1$\beta$, $P = 0.011$ and 0.008; IL-6, $P = 0.040$ and 0.024; IL-22, $P = 0.024$ and 0.041). *Scnn1b*-Tg mice also produced increased levels of IL-17 on day 3 postinfection ($P = 0.025$). Production of TNF-$\alpha$ and TGF-$\beta$ was not significantly affected by *P. aeruginosa* infection and did not differ between *Scnn1b*-Tg and wild-type mice. By day 7 postinfection, cytokine levels were similar to baseline, with the exception of wild-type mice continuing to produce slightly elevated levels of IL-1$\beta$ ($P = 0.018$).

**Infection with *P. aeruginosa* CF clinical isolates.** As PAO1 is a laboratory-adapted strain of *P. aeruginosa*, *Scnn1b*-Tg and wild-type mice were infected using *P. aeruginosa* isolates from CF patients to determine whether *Scnn1b*-Tg mice were more susceptible than their wild-type littermates. To model the earliest stages of *P. aeruginosa* infections in the CF lung, *Scnn1b*-Tg and wild-type mice were infected with the nonmucoid CF isolates CF001 and CF002, both grown as biofilms. CF001 and CF002, collected as part of previous studies that characterized the early natural history of CF lung disease (44, 45), were from individual 3-month-old and 4-month-old CF patients, respectively. Both isolates were collected via bronchoalveolar lavage. Similar to PAO1, both CF001 and CF002 exhibited colonization of the airways of *Scnn1b*-Tg mice on day 7, whereas they were cleared from the lungs of wild-type mice ($P = 0.001$ and 0.068) (Fig. 4). The bacterial burdens recovered from mice infected with PAO1 were not significantly

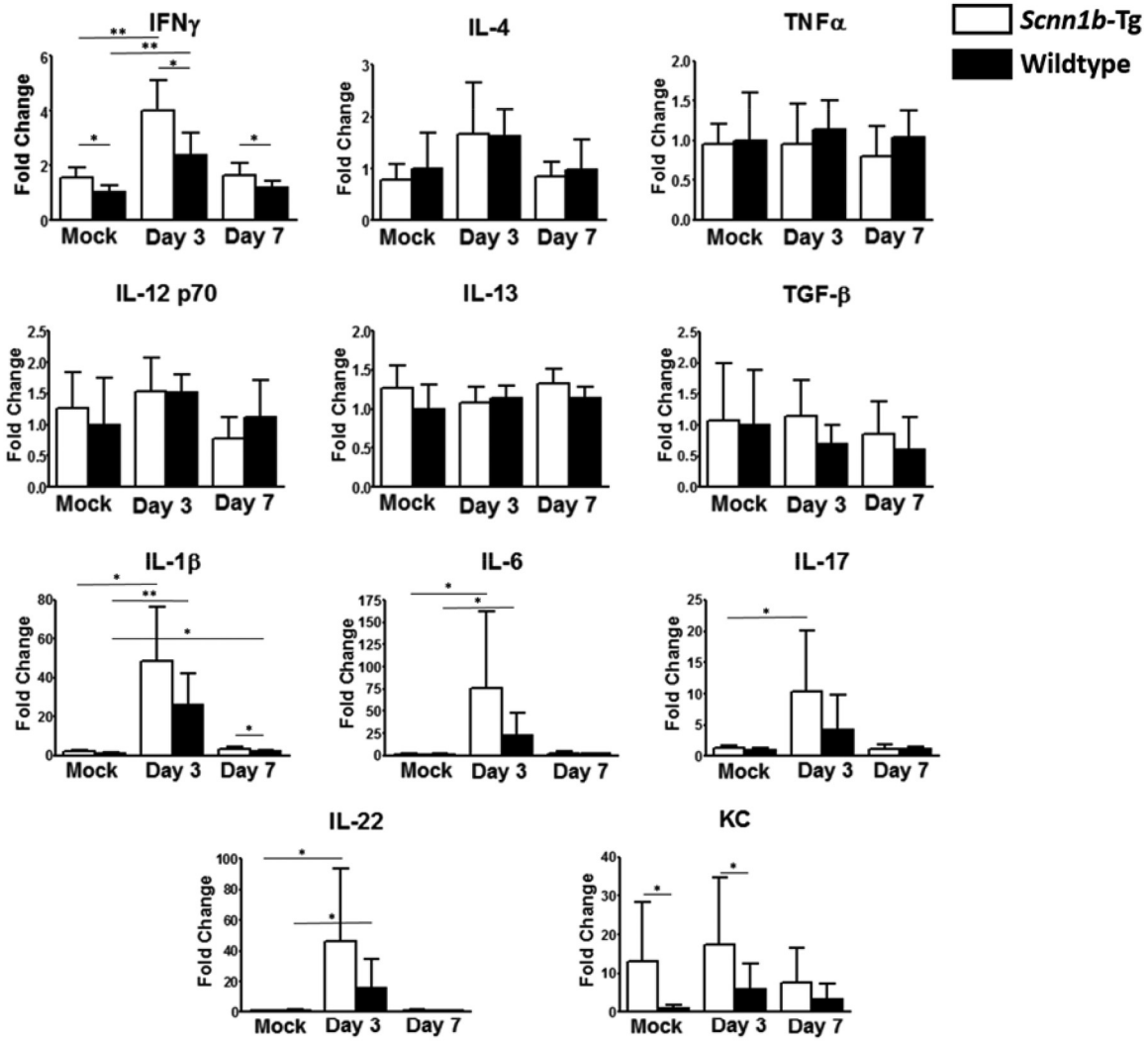


**FIG 3** PAO1 infection elicits an early Th17-type response. The cytokine response to PAO1 infection was measured on days 3 and 7 postinfection in lung homogenates using Luminex multianalyte assays. Data are expressed as fold change relative to wild-type mock-infected mice. Bars represent means with standard deviations. Differences between groups were analyzed with two-tailed unpaired *t* tests (4 to 11 mice per group). *, $P < 0.05$; **, $P < 0.01$.

different from those in mice infected with CF001 or CF002 ($P = 0.107$ and $P = 0.142$, respectively).

To model CF lung infection with a *P. aeruginosa* isolate that displayed specific CF lung adaptations, including mucoidy, mice were infected with $1 \times 10^5$ CFU of the CF isolate CF1188, a mucoid isolate from an 18-month-old CF patient. In contrast to infections with PAO1 and the nonmucoid early CF isolates CF001 and CF002, mice infected with CF1188 displayed decreased signs of disease in the first 3 days after infection (less ruffled fur, no hunched posture); however, CF1188-infected *Scnn1b*-Tg mice gradually lost weight during the course of the infection. Wild-type BALB/c mice did not show significant weight loss (data not shown). On day 7, a geometric mean of $1.5 \times 10^8$ CFU/g of lung was recovered from *Scnn1b*-Tg mice, whereas the geometric mean in BALB/c mice was below the limit of detection ($P < 0.0001$) (Fig. 4). In two of six *Scnn1b*-Tg mice, bacteria were recovered from the kidneys, indicating dissemination of CF1188 from the lungs of *Scnn1b*-Tg mice, which did not occur in wild-type mice. Repeated infections with CF1188 yielded similar results (data not shown).

Cytokine production in the lungs of mice infected with all three CF clinical isolates was compared to that in mice infected with PAO1 on day 7 postinfection. Generally,

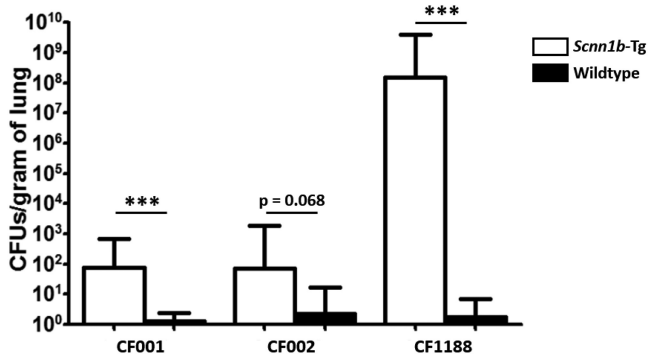


**FIG 4** *Scnn1b*-Tg mice carry higher bacterial burdens when infected with CF *P. aeruginosa* isolates. *Scnn1b*-Tg and wild-type mice were intranasally infected with the CF isolate CF001, CF002, or CF1188 and sacrificed on day 7 postinfection. Bars represent geometric means with 95% confidence intervals. CFU values were log transformed and analyzed using two-tailed unpaired *t* tests (CF001 data are from 2 independent infections with 16 *Scnn1b*-Tg mice and 16 wild-type mice; CF002 data are from 1 infection with 9 *Scnn1b*-Tg mice and 7 wild-type mice; CF1188 data are from 1 infection with 6 *Scnn1b*-Tg mice and 8 wild-type mice). The limit of detection is 100 CFU/g of lung. ***, $P < 0.001$.

mice infected with the nonmucoid early CF isolates, CF001 and CF002, mounted cytokine responses similar to those of mice infected with PAO1, while mice infected with the mucoid CF isolate CF1188 generated increased cytokine responses. As observed in PAO1-infected *Scnn1b*-Tg mice on day 7, no significant increases in tumor necrosis factor alpha (TNF-$\alpha$), IL-1$\beta$, IFN-$\gamma$, IL-13, IL-17, or IL-22 were observed in *Scnn1b*-Tg mice infected with CF001 or CF002. In contrast, *Scnn1b*-Tg mice infected with either CF001, CF002, or CF1188 produced significantly more KC than mock-infected controls ($P = 0.013$, 0.035, and 0.006, respectively). *Scnn1b*-Tg mice infected with the mucoid isolate CF1188 produced significantly more IL-1$\beta$, IL-13, IL-17, IL-22, and KC than mice infected with PAO1, CF001, or CF002 ($P = 0.005$, 0.023, 0.010, 0.010, and 0.001, respectively) (Fig. 5). In wild-type mice, infection with CF isolates resulted in a significant increase in IL-13, compared to infection with PAO1 ($P = 0.007$), and decreases in the production of IL-1$\beta$, TNF-$\alpha$, IL-17, and KC ($P = 0.004$, 0.006, 0.016, and 0.021, respectively).

**Histology.** As previously reported (37), *Scnn1b*-Tg mouse lungs were characterized by mucus accumulation in the bronchioles, neutrophilic infiltration, and enlarged alveoli, compared to those of wild-type littermates, even in the absence of infection (Fig. S3). On day 7 postinfection, H&E-stained *Scnn1b*-Tg mouse lungs showed slightly increased immune infiltration into the bronchioles (Fig. 6). Both wild-type and *Scnn1b*-Tg mice displayed alveolar septal thickening and cellular debris in the alveoli in response to PAO1 infection. *Scnn1b*-Tg mice infected with CF001 and CF002 showed similar signs of inflammation on day 7 (Fig. S4). Both neutrophils and alveolar macrophages were present in the mucus in *Scnn1b*-Tg mice, and individual bacteria and small bacterial aggregates were located in the bronchioles and alveoli using immunohistochemistry (Fig. S5). In contrast, *Scnn1b*-Tg mice infected with CF1188 showed extensive immune cell infiltration into the bronchioles and some alveoli. Wild-type mice, on the other hand, showed minimal pathology (Fig. 7). In order to locate CF1188 in the airway, lung sections were stained with anti-*P. aeruginosa* antibodies. Aggregates of bacteria were identified both in bronchioles and in alveoli, extending to the edge of the lung parenchyma (Fig. 8; Fig. S5). Although individual bacteria were observed, CF1188 was primarily found in aggregates that ranged in size from approximately 2 to 20 $\mu$m in diameter.

## DISCUSSION

Here, we showed the applicability of *Scnn1b*-Tg BALB/c mice as a model of *P. aeruginosa* colonization of the CF lung. In these studies, *Scnn1b*-Tg mice remained infected longer and showed increased neutrophilic infiltration into the bronchioles,

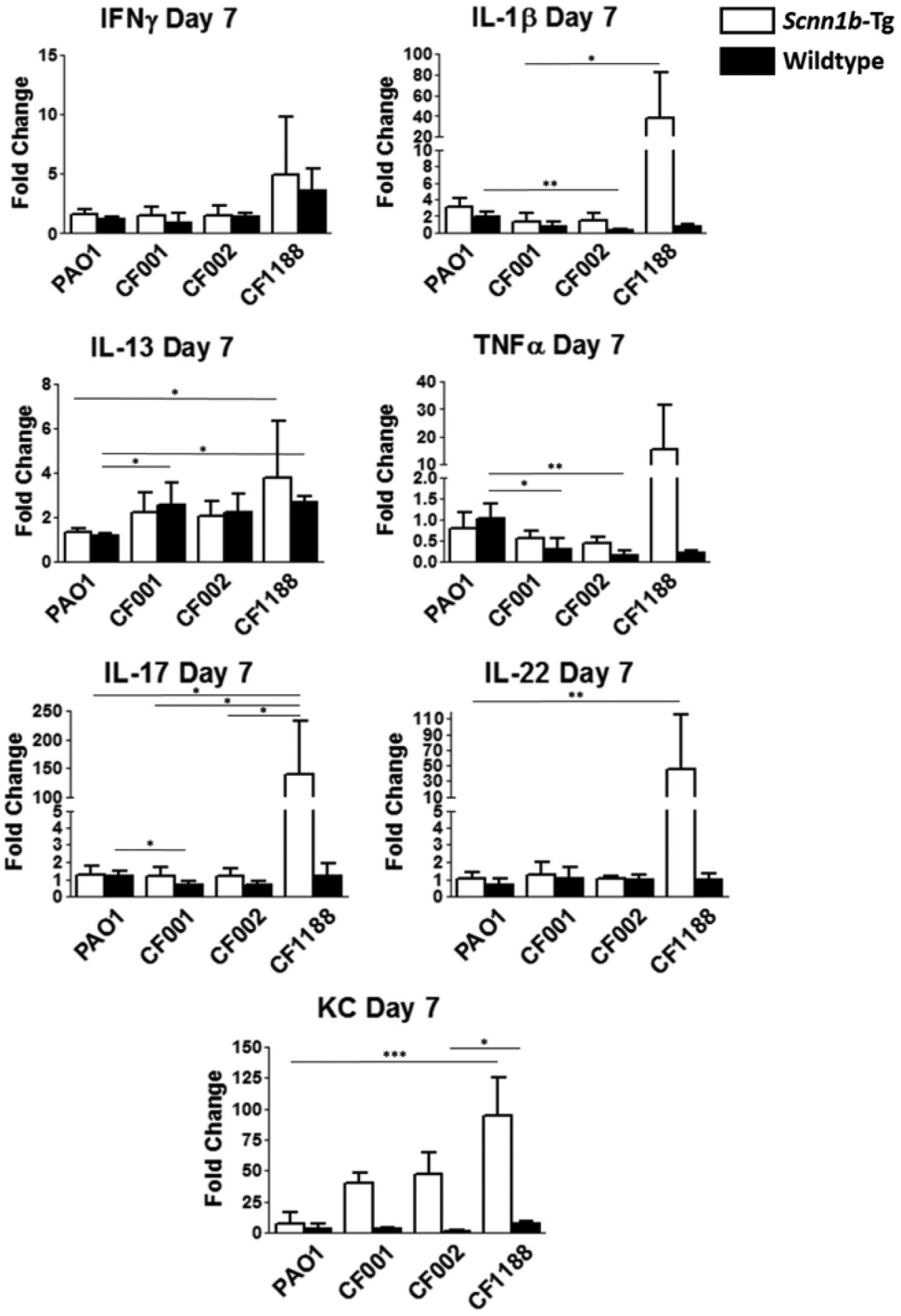


**FIG 5** *Scnn1b*-Tg mice generate elevated cytokine responses after infection with CF1188. Bars represent means with standard deviations. Differences between groups were analyzed with Kruskal-Wallis tests and Dunn's multiple-comparison *post hoc* tests. Horizontal bars and asterisks represent the results of Dunn's multiple-comparison tests (5 to 6 mice per group). *, $P < 0.05$; **, $P < 0.01$; ***, $P < 0.001$.

compared to wild-type mice. In addition, *Scnn1b*-Tg mice generated Th17-type cytokines in response to infection, which is consistent with observed responses in CF patients.

We found that PAO1 consistently colonized the lungs of *Scnn1b*-Tg mice when it was grown as a biofilm prior to infection rather than planktonically. The formation of bacterial biofilms in the lungs of CF patients plays an important role in the persistence

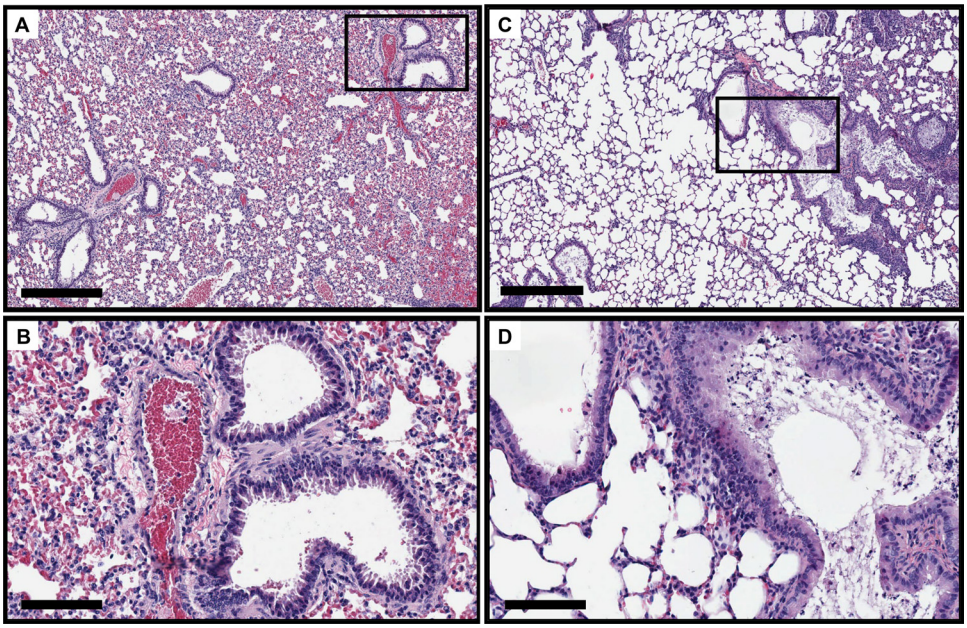


**FIG 6** PAO1 infection elicits increased immune infiltration in the bronchioles of *Scnn1b*-Tg mice (C and D) on day 7 postinfection. Wild-type mice (A and B) display signs of inflammation but lack excessive neutrophil recruitment. Bars, 400 $\mu$m (A and C) and 100 $\mu$m (B and D).

of lung infections, and bacteria have been observed in microcolonies and aggregates in sputum (46, 47). Biofilm growth offers multiple advantages to a pathogen, such as the ability to better evade the host immune response and tolerate antibiotic exposure. Although aggressive antibiotic treatment can be beneficial in treating CF patients' airway disease, chronic *P. aeruginosa* infections are not eradicated by antibiotic treatment. Biofilm-related antibiotic tolerance has been attributed to reduced penetration into the biofilm and decreased metabolic activity of bacteria within the biofilm (48).

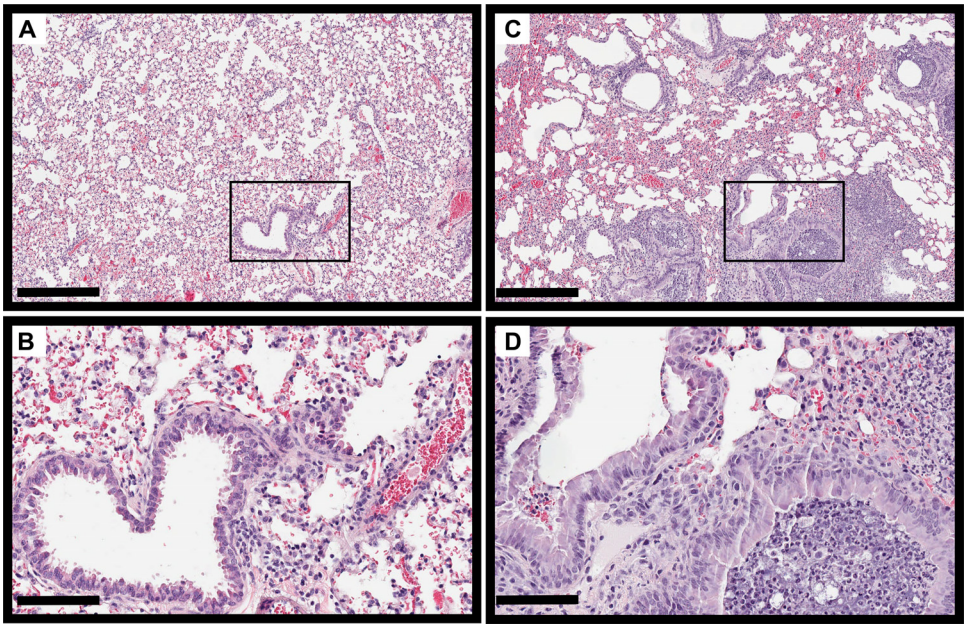


**FIG 7** *Scnn1b*-Tg mice show pronounced immune cell infiltration into the bronchioles on day 7 following infection with CF1188 (C and D). Wild-type mice show minimal pathology (A and B). Bars, 400 $\mu$m (A and C) and 100 $\mu$m (B and D).

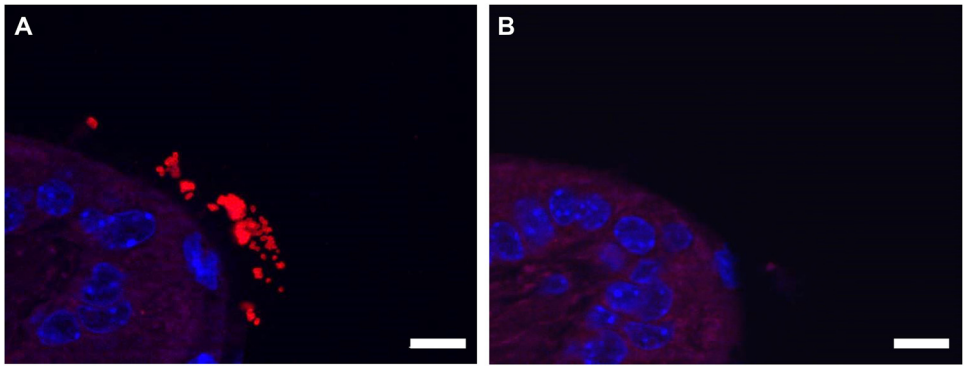


**FIG 8** (A) CF1188 (red) formed aggregates in the lungs of *Scnn1b*-Tg mice, visualized using immunohistochemistry. Bacteria were localized using an anti-*P. aeruginosa* antibody with a DAPI counterstain. (B) Negative control. Bar, 10 $\mu$m.

Although the role of biofilms in maintaining chronic disease is well established, a potential role for bacterial aggregates in the initiation of disease is not as well understood. *Vibrio cholerae*, for example, is more infectious as a biofilm than it is as a planktonic organism (49, 50), but the physical structure of the aggregate has been found to be dispensable (51). Future studies will address the features of the PAO1 biofilm that enhance the colonization of *Scnn1b*-Tg mouse lungs.

We extended these studies by using *P. aeruginosa* isolates (CF001, CF002, and CF1188) collected from young patients with CF. When *P. aeruginosa* colonizes the CF lung, it encounters a stressful environment and must evade the immune response and survive exposure to antibiotics (52) and osmotic and oxidative stresses (53, 54). To survive and establish a chronic infection, *P. aeruginosa* must adapt to the CF lung environment. Several recurring adaptations have been identified from genotypic and phenotypic studies of CF isolates. For example, *P. aeruginosa* becomes nonmotile (55) and hypermutable, loses quorum sensing (56), and becomes increasingly antibiotic resistant (57). The development of mucoidy is especially important in the transition to a chronic infection in CF (58).

All three clinical isolates used in this study were obtained from individual patients 18 months old or younger; however, CF1188 is mucoid and CF001 and CF002 are nonmucoid. Infections in *Scnn1b*-Tg mice with PAO1, CF001, and CF002 were similar with regard to the bacterial numbers recovered from the lungs and the cytokine response at day 7 postinfection. *Scnn1b*-Tg mice carried higher bacterial burdens than wild-type mice when infected with *P. aeruginosa* CF isolates. Notably, infection with the mucoid isolate CF1188 resulted in the highest bacterial burdens ($>10^8$ CFU) in *Scnn1b*-Tg mice on day 7. Correspondingly, *Scnn1b*-Tg mice infected with CF1188 mounted increased cytokine responses, compared to mice infected with PAO1, CF001, or CF002. On histological examination of hematoxylin-and-eosin (H&E)-stained lungs, *Scnn1b*-Tg mice infected with PAO1, CF001, or CF002 all displayed signs of inflammation, including neutrophil infiltration, lymphoid hyperplasia, the appearance of foamy alveolar macrophages, and thickening of the alveolar septa. *Scnn1b*-Tg mice infected with CF1188 additionally showed extensive immune cell infiltration into the bronchioles. Although CF1188 proliferated in the *Scnn1b*-Tg lung and caused dramatic cytokine responses, wild-type mice cleared CF1188 infections and showed minimal pathology, a dichotomy that illustrates the significance of CF-like pathology in permitting mucoid *P. aeruginosa* to establish lung infections.

In *Scnn1b*-Tg mice infected with PAO1, IL-17 was elevated in lung homogenate on day 3 but had returned to baseline by day 7, suggesting that innate-like cells could be responsible for much of the production of IL-17. Invariant natural killer cells, type III innate lymphoid cells, and $\gamma\delta$ T cells have all been shown to secrete IL-17 and are present at mucosal surfaces (59, 60). During infection with CF1188, IL-17, IL-22, and KC

remained elevated at day 7, likely due to the high bacterial load in the lung. IL-17-family cytokines have been found in the sputum of CF patients during exacerbations (43), and neutrophils from *P. aeruginosa*-infected CF patients produce IL-17 during infections (61). As previously shown in other murine models, the IL-17–IL-22 axis plays an important role in both the control of infections and the repair of epithelium following inflammation. Mice deficient in IL-17 or IL-23 production are more vulnerable to respiratory infection with bacterial (59, 60) and fungal (62) pathogens; however, in CFTR knockout mice, the administration of IL-17-blocking antibodies prior to infection with *P. aeruginosa*-laden agarose beads resulted in decreased lung pathology and less weight loss (63). In the highly inflamed CF lung, blocking the actions of IL-17 to decrease neutrophil infiltration and control inflammation is a potential therapeutic strategy.

In *Scnn1b*-Tg mice infected with PAO1, *P. aeruginosa* was primarily identified in the bronchioles as individual organisms. In contrast, in the lungs of *Scnn1b*-Tg mice infected with the mucoid isolate CF1188, aggregates of CF1188 were found in both bronchioles and alveoli. The observed CF1188 aggregates were approximately 20 $\mu$m across their longest axis. Infecting mice with a mucoid CF isolate appears to produce bacterial aggregates similar in size to those observed in both the alginate bead model and in CF patients. In the alginate bead model of *P. aeruginosa* lung infections, aggregates are approximately 23 to 342 $\mu m^2$ (64). *P. aeruginosa* aggregates have been reported to range in size from 4 to 3,227 $\mu m^2$ in explanted CF patient lungs (65), and in a review comparing characteristics of biofilms in human infections and *in vitro* models, aggregates in CF patients were reported to be in the range of 5 to 100 $\mu$m long (66).

This study had several limitations. Although *Scnn1b*-Tg mice maintained *P. aeruginosa* infections for 7 to 12 days, we did not assess whether an infection would continue for a longer duration. By day 12 postinfection, half of the infected *Scnn1b*-Tg mice had cleared the infection, but it is possible that some of the remaining infected mice would have maintained the infection longer. Because *Scnn1b*-Tg mice do not carry CFTR mutations, this model is also limited in its utility for the study of CFTR-targeting therapies.

Advantages of utilizing *Scnn1b*-Tg mice as models of CF lung infections include the ability to study microbial pathogenesis and the host immune response in a mucus-obstructed lung that recapitulates many of the features of CF lung pathology. This model can potentially be adapted to evaluate antibiotics or immunomodulatory treatments or to assess virulence of isolates in a CF-like lung. Future studies will expand this model to characterize other important CF-associated pathogens and study bacterial interactions in polymicrobial infections.

## MATERIALS AND METHODS

**Animals.** Wanda O'Neal and the Marsico Lung Institute Mouse Models Core at the University of North Carolina School of Medicine generously provided male *Scnn1b*-Tg (also known as $\beta$-ENaC) (37) BALB/c mice for the initiation of the colony. *Scnn1b*-Tg mice are reviewed in references 67 and 68. Female BALB/c mice were purchased from Taconic Biosciences (Rensselaer, NY) as breeders. *Scnn1b*-Tg mice were bred as hemizygotes, and their wild-type BALB/c littermates served as controls. Pups were genotyped by PCR of genomic tail DNA as previously described (37). DNA was extracted using a DNeasy blood and tissue kit (Qiagen, Hilden, Germany) per the manufacturer's instructions. All mice were housed in the animal facility at the University of Maryland School of Dentistry. The Institutional Animal Care and Use Committee at the University of Maryland, Baltimore, MD, approved the experiments.

**Bacterial strains and cultures.** Bacteria were stored at −80°C in 20% glycerol (vol/vol). Thomas Bjarnsholt (University of Copenhagen) provided the isolate of PAO1 (69) used in this study. CF isolates were from young CF patients enrolled in a study at the Children's Hospital and Regional Medical Center in Seattle, Washington (44). The children were younger than 15 months old at enrollment and were followed until age 3. *P. aeruginosa* isolates were obtained from bronchoalveolar lavage fluid or oropharyngeal cultures. Strain information for all *P. aeruginosa* isolates used for the study is listed in Table 1.

Bacteria were maintained on tryptic soy agar (TSA; Sigma-Aldrich Corporation, St. Louis, MO) plates and cultured overnight in tryptic soy broth (TSB; Sigma-Aldrich) at 37°C (shaking at 200 rpm). To generate biofilm-grown cultures, the overnight cultures were diluted 1:100 and incubated for an additional 3 h to reach mid-log phase, and then 10 $\mu$l of the subculture was spiked into wells of a 6-well polystyrene tissue culture plate (Corning Inc., Corning, NY) with 3 ml TSB. The plate was cultured overnight at 37°C without

**TABLE 1** Characteristics of strains used in this study

| Strain | Origin | Patient no. | Mucoidy | Reference(s) |
|---|---|---|---|---|
| PAO1 | Wound; Melbourne, Australia, 1954 | NA[a] | No | 69 |
| CF001 | CF patient; 3 months | 003 | No | 44, 45 |
| CF002 | CF patient; 4 months | 001 | No | 44, 45 |
| CF1188 | CF patient; 18 months | 008 | Yes | 44, 45 |

[a]NA, not applicable.

shaking. The resulting biofilm and planktonic populations were harvested together from each well of the plate; thus, the biofilm inoculum was a mixed population containing both planktonic bacteria and biofilm aggregates. The bacteria were centrifuged (4,200 $\times$ *g* for 10 min), washed with 10 ml phosphate-buffered saline (PBS; Sigma-Aldrich), and then centrifuged again. The pellet was resuspended in PBS to an optical density at 600 nm ($OD_{600}$) of 0.065 $\pm$ 0.003 (for PAO1, CF001, and CF002), which had been previously determined to correspond to a bacterial concentration of approximately $7 \times 10^7$ CFU/ml. CF1188 was capable of establishing an infection with a lower-concentration inoculum, so the inoculum was diluted an additional 30-fold from an $OD_{600}$ of 0.065. The biofilm inoculum was vortexed vigorously for 1 min to disrupt visible bacterial aggregates. Following infection, the remaining inoculum was homogenized for 1 min with a Kinematica Polytron PT1200E tissue homogenizer (Kinematic Inc., Lucerne, Switzerland). The inoculum was serially diluted and plated in triplicate to confirm the bacterial concentration. The planktonic inoculum was prepared by growing an overnight culture in TSB (shaking at 200 rpm), diluting it 1:100, and incubating it for an additional 3 h. The subcultures were centrifuged and washed with PBS in the same manner as the biofilm inocula and then diluted to the same $OD_{600}$. The preparation of the biofilm and planktonic inocula is summarized in Fig. S1A.

**Lung infection model.** Seven to 10-week-old male and female mice were anesthetized with inhaled isoflurane (VetOne, Boise, ID), intraperitoneal ketamine (Putney Inc., Portland, ME), and xylazine (VetOne) (100 to 150 mg/kg of body weight and 10 to 16 mg/kg, respectively) and then infected intranasally with *P. aeruginosa* suspended in 50 $\mu$l PBS. Mice were euthanized by $CO_2$ narcosis and cervical dislocation on days 3, 7, and 12 postinfection. Mock-infected mice were anesthetized in the same manner, intranasally inoculated with 50 $\mu$l sterile PBS, and sacrificed on day 3 after mock infection. Mice were monitored daily for the duration of the infection, and moribund mice were euthanized. Only surviving mice were included in CFU calculations, calculations of percentage of mice infected, and cytokine analysis.

**Quantitative bacteriology.** Right lungs were excised aseptically, weighed, and homogenized in PBS (3 ml PBS/g lung tissue) using a Kinematica Polytron PT1200E tissue homogenizer. Lung homogenate was serially diluted and plated in triplicate on TSA and on *Pseudomonas*-selective agar (CHROMagar, Paris, France) to determine bacterial load. Plates were incubated at 37°C overnight. Colonies were counted and presented as CFU per gram of lung to standardize values across different mouse sizes. The limit of detection was 100 CFU/g.

**Cytokine production.** Right lungs were weighed and homogenized in PBS (3 ml/g lung tissue) containing a cOmplete protease inhibitor cocktail (Roche, Basel, Switzerland) and 2% bovine serum albumin (BSA; AmericanBio Inc., Canton, MA). The lung homogenate was centrifuged at 4,200 $\times$ *g* for 10 min at 4°C, and the supernatant was stored at $-20$°C until analysis. The University of Maryland Cytokine Core Laboratory performed all cytokine assays using a Luminex multianalyte system.

**Histology.** Left lungs were removed aseptically and harvested directly into 10% (wt/vol) neutral buffered formalin (Sigma-Aldrich). After a minimum of 48 h in formalin at room temperature, the lungs were embedded in paraffin wax and cut into 5-$\mu$m-thick sections, followed by hematoxylin-and-eosin (H&E) staining. Sectioning and H&E staining were performed by the Pathology, EM, and Histology Laboratory at the University of Maryland. Slides were analyzed by workers who were blind to the mouse genotype and infection status.

Immunohistochemistry was used to locate *P. aeruginosa* in the airways of infected mice. In brief, paraffin-embedded lung sections were deparaffinized and rehydrated in water before undergoing antigen retrieval (sodium citrate buffer, pH 6.0) at 60°C overnight. Nonspecific staining was blocked with 2% BSA and 0.1% Triton X-100, and slides were stained overnight with a rabbit anti-*P. aeruginosa* antibody (Abcam 68538; Abcam, Cambridge, United Kingdom) at a 1:400 dilution. The slides were washed, stained with a goat anti-rabbit secondary antibody conjugated to Texas Red (Abcam 6719) at a 1:400 dilution, and then counterstained with DAPI (4′,6-diamidino-2-phenylindole) Prolong Diamond (Invitrogen, Carlsbad, CA). Mock-infected mice and slides from infected mice with the primary antibody replaced with an additional blocking step served as negative controls. Slides were visualized using a Zeiss Axio Imager fluorescence microscope equipped with an ApoTome module.

**Statistical analysis.** GraphPad Prism 5.0 (GraphPad Software, Inc., San Diego, CA) was used for graph creation and statistical analysis. *t* tests were used to analyze normally distributed data. Nonnormally distributed data were log transformed prior to performance of *t* tests. Kruskal-Wallis tests with Dunn's multiple comparison *post hoc* tests were used to assess differences between more than two groups when variances were not equal. Differences in mortality were assessed with log-rank tests. Fold changes in cytokine expression were calculated for each mouse compared to mock-infected wild-type mice. A *P* value less than 0.05 was considered statistically significant.

## SUPPLEMENTAL MATERIAL

Supplemental material is available online only.

**SUPPLEMENTAL FILE 1**, PDF file, 1 MB.

## ACKNOWLEDGMENTS

This research was funded by grants to J.M.H. and R.K.E. from the Cystic Fibrosis Foundation (Ernst18G0 and Ernst18I0). K.B. was a trainee supported by a training grant from the National Institute of Allergy and Infectious Diseases (Institutional Training Grant T32AI007540).

The content is the responsibility of the authors and is not necessarily endorsed by the Cystic Fibrosis Foundation or the National Institutes of Health.

We thank Francesca Gardner for her editing assistance and Kimberly Filcek for microscopy assistance.

M.E.S. passed away before completion of the project. We thank him for his ideas and support.

## REFERENCES

1. Donlan RM, Costerton JW. 2002. Biofilms: survival mechanisms of clinically relevant microorganisms. Clin Microbiol Rev 15:167–193. https://doi.org/10.1128/cmr.15.2.167-193.2002.
2. Rybtke M, Hultqvist LD, Givskov M, Tolker-Nielsen T. 2015. *Pseudomonas aeruginosa* biofilm infections: community structure, antimicrobial tolerance and immune response. J Mol Biol 427:3628–3645. https://doi.org/10.1016/j.jmb.2015.08.016.
3. Jackson AE, Southern PM, Pierce AK, Fallis BD, Sanford JP. 1967. Pulmonary clearance of gram-negative bacilli. J Lab Clin Med 69:833–841.
4. Southern PM, Jr, Mays BB, Pierce AK, Sanford JP. 1970. Pulmonary clearance of *Pseudomonas aeruginosa*. J Lab Clin Med 76:548–559.
5. Feldman M, Bryan R, Rajan S, Scheffler L, Brunnert S, Tang H, Prince A. 1998. Role of flagella in pathogenesis of *Pseudomonas aeruginosa* pulmonary infection. Infect Immun 66:43–51. https://doi.org/10.1128/IAI.66.1.43-51.1998.
6. Tang H, Kays M, Prince A. 1995. Role of *Pseudomonas aeruginosa* pili in acute pulmonary infection. Infect Immun 63:1278–1285. https://doi.org/10.1128/IAI.63.4.1278-1285.1995.
7. Lee VT, Smith RS, Tummler B, Lory S. 2005. Activities of *Pseudomonas aeruginosa* effectors secreted by the type III secretion system *in vitro* and during infection. Infect Immun 73:1695–1705. https://doi.org/10.1128/IAI.73.3.1695-1705.2005.
8. Saint-Criq V, Villeret B, Bastaert F, Kheir S, Hatton A, Cazes A, Xing Z, Sermet-Gaudelus I, Garcia-Verdugo I, Edelman A, Sallenave JM. 2018. *Pseudomonas aeruginosa* LasB protease impairs innate immunity in mice and humans by targeting a lung epithelial cystic fibrosis transmembrane regulator-IL-6-antimicrobial-repair pathway. Thorax 73:49–61. https://doi.org/10.1136/thoraxjnl-2017-210298.
9. Lau GW, Ran H, Kong F, Hassett DJ, Mavrodi D. 2004. *Pseudomonas aeruginosa* pyocyanin is critical for lung infection in mice. Infect Immun 72:4275–4278. https://doi.org/10.1128/IAI.72.7.4275-4278.2004.
10. Recinos DA, Sekedat MD, Hernandez A, Cohen TS, Sakhtah H, Prince AS, Price-Whelan A, Dietrich LE. 2012. Redundant phenazine operons in *Pseudomonas aeruginosa* exhibit environment-dependent expression and differential roles in pathogenicity. Proc Natl Acad Sci U S A 109:19420–19425. https://doi.org/10.1073/pnas.1213901109.
11. Starke JR, Edwards MS, Langston C, Baker CJ. 1987. A mouse model of chronic pulmonary infection with *Pseudomonas aeruginosa* and *Pseudomonas cepacia*. Pediatr Res 22:698–702. https://doi.org/10.1203/00006450-198712000-00017.
12. Pedersen SS, Shand GH, Hansen BL, Hansen GN. 1990. Induction of experimental chronic *Pseudomonas aeruginosa* lung infection with *P aeruginosa* entrapped in alginate microspheres. APMIS 98:203–211. https://doi.org/10.1111/j.1699-0463.1990.tb01023.x.
13. Chandler JD, Min E, Huang J, Nichols DP, day BJ. 2013. Nebulized thiocyanate improves lung infection outcomes in mice. Br J Pharmacol 169:1166–1177. https://doi.org/10.1111/bph.12206.
14. Nichols DP, Jiang D, Happoldt C, Berman R, Chu HW. 2015. Therapeutic effects of alpha1-antitrypsin on *Psedumonas* [sic] *aeruginosa* infection in ENaC transgenic mice. PLoS One 10:e0141232. https://doi.org/10.1371/journal.pone.0141232.
15. Cigana C, Lore NI, Riva C, De Fino I, Spagnuolo L, Sipione B, Rossi G, Nonis A, Cabrini G, Bragonzi A. 2016. Tracking the immunopathological response to *Pseudomonas aeruginosa* during respiratory infections. Sci Rep 6:21465. https://doi.org/10.1038/srep21465.
16. Lore NI, Veraldi N, Riva C, Sipione B, Spagnuolo L, De Fino I, Melessike M, Calzi E, Bragonzi A, Naggi A, Cigana C. 2018. Synthesized heparan sulfate competitors attenuate *Pseudomonas aeruginosa* lung infection. Int J Mol Sci 19:207. https://doi.org/10.3390/ijms19010207.
17. Cutone A, Lepanto MS, Rosa L, Scotti MJ, Rossi A, Ranucci S, De Fino I, Bragonzi A, Valenti P, Musci G, Berlutti F. 2019. Aerosolized bovine lactoferrin counteracts infection, inflammation and iron dysbalance in a cystic fibrosis mouse model of *Pseudomonas aeruginosa* chronic lung infection. Int J Mol Sci 20:2128. https://doi.org/10.3390/ijms20092128.
18. Moser C, Johansen HK, Song Z, Hougen HP, Rygaard J, Hoiby N. 1997. Chronic *Pseudomonas aeruginosa* lung infection is more severe in Th2 responding BALB/c mice compared to Th1 responding C3H/HeN mice. APMIS 105:838–842. https://doi.org/10.1111/j.1699-0463.1997.tb05092.x.
19. Frederiksen B, Lanng S, Koch C, Hølby N. 1996. Improved survival in the Danish center-treated cystic fibrosis patients: results of aggressive treatment. Pediatr Pulmonol 21:153–158. https://doi.org/10.1002/(SICI)1099-0496(199603)21:3<153::AID-PPUL1>3.0.CO;2-R.
20. FitzSimmons SC. 1993. The changing epidemiology of cystic fibrosis. J Pediatr 122:1–9. https://doi.org/10.1016/s0022-3476(05)83478-x.
21. Langton Hewer SC, Smyth AR. 2017. Antibiotic strategies for eradicating *Pseudomonas aeruginosa* in people with cystic fibrosis. Cochrane Database Syst Rev 4:CD004197. https://doi.org/10.1002/14651858.CD004197.pub5.
22. Marvig RL, Sommer LM, Molin S, Johansen HK. 2015. Convergent evolution and adaptation of *Pseudomonas aeruginosa* within patients with cystic fibrosis. Nat Genet 47:57–64. https://doi.org/10.1038/ng.3148.
23. Damkiær S, Yang L, Molin S, Jelsbak L. 2013. Evolutionary remodeling of global regulatory networks during long-term bacterial adaptation to human hosts. Proc Natl Acad Sci U S A 110:7766–7771. https://doi.org/10.1073/pnas.1221466110.
24. Doggett RG. 1969. Incidence of mucoid *Pseudomonas aeruginosa* from clinical sources. Appl Microbiol 18:936–937. https://doi.org/10.1128/AEM.18.5.936-937.1969.
25. Reynolds HY, Di Sant'Agnese PA, Zierdt CH. 1976. Mucoid *Pseudomonas aeruginosa*. A sign of cystic fibrosis in young adults with chronic pulmonary disease? JAMA 236:2190–2192. https://doi.org/10.1001/jama.1976.03270200028024.
26. Pedersen SS. 1992. Lung infection with alginate-producing, mucoid *Pseudomonas aeruginosa* in cystic fibrosis. APMIS Suppl 28:1–79.
27. Mayer-Hamblett N, Rosenfeld M, Gibson RL, Ramsey BW, Kulasekara HD, Retsch-Bogart GZ, Morgan W, Wolter DJ, Pope CE, Houston LS, Kulasekara BR, Khan U, Burns JL, Miller SI, Hoffman LR. 2014. *Pseudomonas aeruginosa in vitro* phenotypes distinguish cystic fibrosis infection stages

and outcomes. Am J Respir Crit Care Med 190:289–297. https://doi.org/10.1164/rccm.201404-0681OC.
28. Limoli DH, Whitfield GB, Kitao T, Ivey ML, Davis MR, Grahl N, Hogan DA, Rahme LG, Howell PL, O'Toole GA, Goldberg JB. 2017. *Pseudomonas aeruginosa* alginate overproduction promotes coexistence with *Staphylococcus aureus* in a model of cystic fibrosis respiratory infection. mBio 8:e00186-17. https://doi.org/10.1128/mBio.00186-17.
29. Hentzer M, Teitzel GM, Balzer GJ, Heydorn A, Molin S, Givskov M, Parsek MR. 2001. Alginate overproduction affects *Pseudomonas aeruginosa* biofilm structure and function. J Bacteriol 183:5395–5401. https://doi.org/10.1128/jb.183.18.5395-5401.2001.
30. Pier GB, Coleman F, Grout M, Franklin M, Ohman DE. 2001. Role of alginate O acetylation in resistance of mucoid *Pseudomonas aeruginosa* to opsonic phagocytosis. Infect Immun 69:1895–1901. https://doi.org/10.1128/IAI.69.3.1895-1901.2001.
31. Simpson JA, Smith SE, Dean RT. 1988. Alginate inhibition of the uptake of *Pseudomonas aeruginosa* by macrophages. J Gen Microbiol 134:29–36. https://doi.org/10.1099/00221287-134-1-29.
32. Henry RL, Mellis CM, Petrovic L. 1992. Mucoid *Pseudomonas aeruginosa* is a marker of poor survival in cystic fibrosis. Pediatr Pulmonol 12:158–161. https://doi.org/10.1002/ppul.1950120306.
33. Delaney SJ, Alton EW, Smith SN, Lunn DP, Farley R, Lovelock PK, Thomson SA, Hume DA, Lamb D, Porteous DJ, Dorin JR, Wainwright BJ. 1996. Cystic fibrosis mice carrying the missense mutation G551D replicate human genotype-phenotype correlations. EMBO J 15:955–963. https://doi.org/10.1002/j.1460-2075.1996.tb00432.x.
34. Zeiher BG, Eichwald E, Zabner J, Smith JJ, Puga AP, McCray PB, Jr, Capecchi MR, Welsh MJ, Thomas KR. 1995. A mouse model for the delta F508 allele of cystic fibrosis. J Clin Invest 96:2051–2064. https://doi.org/10.1172/JCI118253.
35. Stutts MJ, Canessa CM, Olsen JC, Hamrick M, Cohn JA, Rossier BC, Boucher RC. 1995. CFTR as a cAMP-dependent regulator of sodium channels. Science 269:847–850. https://doi.org/10.1126/science.7543698.
36. Mall M, Bleich M, Greger R, Schreiber R, Kunzelmann K. 1998. The amiloride-inhibitable Na+ conductance is reduced by the cystic fibrosis transmembrane conductance regulator in normal but not in cystic fibrosis airways. J Clin Invest 102:15–21. https://doi.org/10.1172/JCI2729.
37. Mall M, Grubb BR, Harkema JR, O'Neal WK, Boucher RC. 2004. Increased airway epithelial Na+ absorption produces cystic fibrosis-like lung disease in mice. Nat Med 10:487–493. https://doi.org/10.1038/nm1028.
38. Johannesson B, Hirtz S, Schatterny J, Schultz C, Mall MA. 2012. CFTR regulates early pathogenesis of chronic obstructive lung disease in betaENaC-overexpressing mice. PLoS One 7:e44059. https://doi.org/10.1371/journal.pone.0044059.
39. Saini Y, Lewis BW, Yu D, Dang H, Livraghi-Butrico A, Del Piero F, O'Neal WK, Boucher RC. 2018. Effect of LysM+ macrophage depletion on lung pathology in mice with chronic bronchitis. Physiol Rep 6:e13677. https://doi.org/10.14814/phy2.13677.
40. Small DM, Brown RR, Doherty DF, Abladey A, Zhou-Suckow Z, Delaney RJ, Kerrigan L, Dougan CM, Borensztajn KS, Holsinger L, Booth R, Scott CJ, Lopez-Campos G, Elborn JS, Mall MA, Weldon S, Taggart CC. 2019. Targeting of cathepsin S reduces cystic fibrosis-like lung disease. Eur Respir J 53:1801523. https://doi.org/10.1183/13993003.01523-2018.
41. Scott DW, Walker MP, Sesma J, Wu B, Stuhlmiller TJ, Sabater JR, Abraham WM, Crowder TM, Christensen DJ, Tarran R. 2017. SPX-101 is a novel epithelial sodium channel-targeted therapeutic for cystic fibrosis that restores mucus transport. Am J Respir Crit Care Med 196:734–744. https://doi.org/10.1164/rccm.201612-2445OC.
42. Terryah ST, Fellner RC, Ahmad S, Moore PJ, Reidel B, Sesma JI, Kim CS, Garland AL, Scott DW, Sabater JR, Carpenter J, Randell SH, Kesimer M, Abraham WM, Arendshorst WJ, Tarran R. 2018. Evaluation of a SPLUNC1-derived peptide for the treatment of cystic fibrosis lung disease. Am J Physiol Lung Cell Mol Physiol 314:L192–L205. https://doi.org/10.1152/ajplung.00546.2016.
43. McAllister F, Henry A, Kreindler JL, Dubin PJ, Ulrich L, Steele C, Finder JD, Pilewski JM, Carreno BM, Goldman SJ, Pirhonen J, Kolls JK. 2005. Role of IL-17A, IL-17F, and the IL-17 receptor in regulating growth-related oncogene-alpha and granulocyte colony-stimulating factor in bronchial epithelium: implications for airway inflammation in cystic fibrosis. J Immunol 175:404–412. https://doi.org/10.4049/jimmunol.175.1.404.
44. Burns JL, Gibson RL, McNamara S, Yim D, Emerson J, Rosenfeld M, Hiatt P, McCoy K, Castile R, Smith AL, Ramsey BW. 2001. Longitudinal assessment of *Pseudomonas aeruginosa* in young children with cystic fibrosis. J Infect Dis 183:444–452. https://doi.org/10.1086/318075.
45. Rosenfeld M, Gibson RL, McNamara S, Emerson J, Burns JL, Castile R, Hiatt P, McCoy K, Wilson CB, Inglis A, Smith A, Martin TR, Ramsey BW. 2001. Early pulmonary infection, inflammation, and clinical outcomes in infants with cystic fibrosis. Pediatr Pulmonol 32:356–366. https://doi.org/10.1002/ppul.1144.
46. Bjarnsholt T, Jensen PO, Fiandaca MJ, Pedersen J, Hansen CR, Andersen CB, Pressler T, Givskov M, Hoiby N. 2009. *Pseudomonas aeruginosa* biofilms in the respiratory tract of cystic fibrosis patients. Pediatr Pulmonol 44:547–558. https://doi.org/10.1002/ppul.21011.
47. Singh PK, Schaefer AL, Parsek MR, Moninger TO, Welsh MJ, Greenberg EP. 2000. Quorum-sensing signals indicate that cystic fibrosis lungs are infected with bacterial biofilms. Nature 407:762–764. https://doi.org/10.1038/35037627.
48. Singh S, Singh SK, Chowdhury I, Singh R. 2017. Understanding the mechanism of bacterial biofilms resistance to antimicrobial agents. Open Microbiol J 11:53–62. https://doi.org/10.2174/1874285801711010053.
49. Huq A, Xu B, Chowdhury MA, Islam MS, Montilla R, Colwell RR. 1996. A simple filtration method to remove plankton-associated *Vibrio cholerae* in raw water supplies in developing countries. Appl Environ Microbiol 62:2508–2512. https://doi.org/10.1128/AEM.62.7.2508-2512.1996.
50. Colwell RR, Huq A, Islam MS, Aziz KM, Yunus M, Khan NH, Mahmud A, Sack RB, Nair GB, Chakraborty J, Sack DA, Russek-Cohen E. 2003. Reduction of cholera in Bangladeshi villages by simple filtration. Proc Natl Acad Sci U S A 100:1051–1055. https://doi.org/10.1073/pnas.0237386100.
51. Tamayo R, Patimalla B, Camilli A. 2010. Growth in a biofilm induces a hyperinfectious phenotype in *Vibrio cholerae*. Infect Immun 78:3560–3569. https://doi.org/10.1128/IAI.00048-10.
52. Maselli DJ, Keyt H, Restrepo MI. 2017. Inhaled antibiotic therapy in chronic respiratory diseases. Int J Mol Sci 18:1062. https://doi.org/10.3390/ijms18051062.
53. Brocker C, Thompson DC, Vasiliou V. 2012. The role of hyperosmotic stress in inflammation and disease. Biomol Concepts 3:345–364. https://doi.org/10.1515/bmc-2012-0001.
54. Hector A, Griese M, Hartl D. 2014. Oxidative stress in cystic fibrosis lung disease: an early event, but worth targeting? Eur Respir J 44:17–19. https://doi.org/10.1183/09031936.00038114.
55. Mahenthiralingam E, Campbell ME, Speert DP. 1994. Nonmotility and phagocytic resistance of *Pseudomonas aeruginosa* isolates from chronically colonized patients with cystic fibrosis. Infect Immun 62:596–605. https://doi.org/10.1128/IAI.62.2.596-605.1994.
56. Hoffman LR, Kulasekara HD, Emerson J, Houston LS, Burns JL, Ramsey BW, Miller SI. 2009. *Pseudomonas aeruginosa* lasR mutants are associated with cystic fibrosis lung disease progression. J Cyst Fibros 8:66–70. https://doi.org/10.1016/j.jcf.2008.09.006.
57. Oliver A, Canton R, Campo P, Baquero F, Blazquez J. 2000. High frequency of hypermutable *Pseudomonas aeruginosa* in cystic fibrosis lung infection. Science 288:1251–1254. https://doi.org/10.1126/science.288.5469.1251.
58. Govan JR, Deretic V. 1996. Microbial pathogenesis in cystic fibrosis: mucoid *Pseudomonas aeruginosa* and *Burkholderia cepacia*. Microbiol Rev 60:539–574. https://doi.org/10.1128/MMBR.60.3.539-574.1996.
59. Bayes HK, Ritchie ND, Evans TJ. 2016. Interleukin-17 is required for control of chronic lung infection caused by *Pseudomonas aeruginosa*. Infect Immun 84:3507–3516. https://doi.org/10.1128/IAI.00717-16.
60. Murakami T, Hatano S, Yamada H, Iwakura Y, Yoshikai Y. 2016. Two types of interleukin 17A-producing gammadelta T cells in protection against pulmonary infection with *Klebsiella pneumoniae*. J Infect Dis 214:1752–1761. https://doi.org/10.1093/infdis/jiw443.
61. Taylor PR, Bonfield TL, Chmiel JF, Pearlman E. 2016. Neutrophils from F508del cystic fibrosis patients produce IL-17A and express IL-23-dependent IL-17RC. Clin Immunol 170:53–60. https://doi.org/10.1016/j.clim.2016.03.016.
62. Rudner XL, Happel KI, Young EA, Shellito JE. 2007. Interleukin-23 (IL-23)-IL-17 cytokine axis in murine *Pneumocystis carinii* infection. Infect Immun 75:3055–3061. https://doi.org/10.1128/IAI.01329-06.
63. Hsu D, Taylor P, Fletcher D, van Heeckeren R, Eastman J, van Heeckeren A, Davis P, Chmiel JF, Pearlman E, Bonfield TL. 2016. Interleukin-17 pathophysiology and therapeutic intervention in cystic fibrosis lung infection and inflammation. Infect Immun 84:2410–2421. https://doi.org/10.1128/IAI.00284-16.
64. Sonderholm M, Kragh KN, Koren K, Jakobsen TH, Darch SE, Alhede M, Jensen PO, Whiteley M, Kuhl M, Bjarnsholt T. 2017. *Pseudomonas aeruginosa* aggregate formation in an alginate bead model system exhibits *in*

*vivo*-like characteristics. Appl Environ Microbiol 83:e00113-17. https://doi.org/10.1128/AEM.00113-17.
65. Kragh KN, Alhede M, Jensen PØ, Moser C, Scheike T, Jacobsen CS, Seier Poulsen S, Eickhardt-Sørensen SR, Trøstrup H, Christoffersen L, Hougen H-P, Rickelt LF, Kühl M, Høiby N, Bjarnsholt T. 2014. Polymorphonuclear leukocytes restrict growth of *Pseudomonas aeruginosa* in the lungs of cystic fibrosis patients. Infect Immun 82:4477–4486. https://doi.org/10.1128/IAI.01969-14.
66. Bjarnsholt T, Alhede M, Alhede M, Eickhardt-Sørensen SR, Moser C, Kühl M, Jensen PØ, Høiby N. 2013. The *in vivo* biofilm. Trends Microbiol 21:466–474. https://doi.org/10.1016/j.tim.2013.06.002.
67. Zhou Z, Duerr J, Johannesson B, Schubert SC, Treis D, Harm M, Graeber SY, Dalpke A, Schultz C, Mall MA. 2011. The ENaC-overexpressing mouse as a model of Cystic Fibrosis lung disease. J Cyst Fibros 10(Suppl 2):S172–S182. https://doi.org/10.1016/S1569-1993(11)60021-0.
68. Lewis BW, Patial S, Saini Y. 2019. Immunopathology of airway surface liquid dehydration disease. J Immunol Res 2019:2180409. https://doi.org/10.1155/2019/2180409.
69. Wu H, Song Z, Givskov M, Doring G, Worlitsch D, Mathee K, Rygaard J, Hoiby N. 2001. *Pseudomonas aeruginosa* mutations in *lasI* and *rhlI* quorum sending systems result in milder chronic lung infection. Microbiology 147:1105–1113. https://doi.org/10.1099/00221287-147-5-1105.